FINAL REPORT

to

NASA LANGLEY

on the project entitled

A LOW LOSS MICROSTRIP ANTENNA FOR RADIOMETRIC APPLICATIONS

submitted by

DR. PARVEEN WAHID
Electrical Engineering Department
Univerity Of Central Florida
Orlando, Florida 32186

May 2000

ABSTRACT

The design and analysis of a series-fed, low-loss, inverted microstrip array antenna, operating at 1.413 GHz is presented. The antenna is composed of two subarrays. Each subarray consists of an equal number of microstrip patches all connected together with microstrip lines. In the first design microstrip array for linear polarization is presented which incorporated a series feeding technique. The next design, which is capable of dual linear polarization (V-polarization and H-polarization), utilizes a corporate feed network for the V-pol and series feed arrangement for the H-pol. The first element of each subarray for H-pol is coaxially fed with a 180° phase difference. This approach ensures a symmetric radiation pattern on broadside in H-pol. For the V-pol two feeds are in the same phase on the two subarrays ensuring a broadside beam in V-pol. The designs presented here are simulated using the IE3D code that utilizes the method of moments. Measured results are compared with simulated results and show good agreement.

CHAPTER 1

INTRODUCTION

Microstrip antennas have been evolved tremendously over the last two decades and come into play every time there is a need for low profile radiators. A microstrip antenna has some certain distinct features such as conformability, compactness, and light weight which are advantages over other antennas. In this project the objective is to design a microstrip antenna array to meet specific radiometer system requirements for the Hydrostar Spacecraft. A radiometric antenna used in remote sensing has to meet some basic requirements such as (i) a narrow beamwidth (ii) low side lobes in all planes to reduce the reception of spurious signals from targets outside the main beam and (iii) very low radiation losses in order to maintain a desired radiometric resolution [1,2].

A series fed array for single linear polarization is first investigated. Next a dual polarized microstrip antenna array is designed. The inverted microstrip configuration was chosen for the designs because this configuration provides less dispersion and dielectric losses than the conventional microstrip antenna configuration [3].

The series fed configuration for the antenna array with single linear polarization is employed to reduce radiation losses. A series configuration minimizes the path length between the elements and thus minimizes ohmic losses [4]. For radiometric applications this reduction of losses makes the series configuration very attractive. The dual polarized microstrip antenna array utilizes both series and corporate feeding technique to achieve the dual polarization. The antenna has series feeding for H-pol (Horizontal Polarization) and corporate feeding for V-pol (Vertical Polarization).

An antenna composed of two subarrays is designed with each subarray consisting of an equal number of microstrip patches connected together with microstrip lines.

Microstrip antennas on substrates of high dielectric constant suffer from very narrow bandwidth (less than 0.5%), low efficiency, and poor radiation pattern due to the presence of unwanted surface waves [5]. To reduce these effects, Rohacell, a substrate with a very small dielectric constant, 1.08, was used along with a superstate of dielectric constant 3.0 (RO3003) to form an inverted antenna. The designs presented are accomplished using the IE3D code [6], which utilizes the method of moments. In Chapter 2, the design procedure of the microstrip antenna array for linear polarization is presented. Chapter 3 describes the design of a dual polarized microstrip antenna array. All experimental and simulated data for the antennas are presented and discussed.

CHAPTER 2

2.0 Design Goals

The microstrip antenna array had to be designed for a frequency of 1.413 GHz. The antenna had to have low loss for radiometric applications and be foldable to allow for transportation into space. The antenna array had to be capable of having dual linear polarization, a radiation pattern with a highly directive beam and side lobe levels below 15 dB. The total length could be around 8-10 feet.

2.1 Foldable linearly polarized microstrip array: Design 1

The configuration in Figure 1 shows one of the subarrays that make up the antenna. It was designed using the software package IE3D for producing highly directive beam on broadside. The patches are tapered in size in order to obtain a low side lobe level and high directivity.

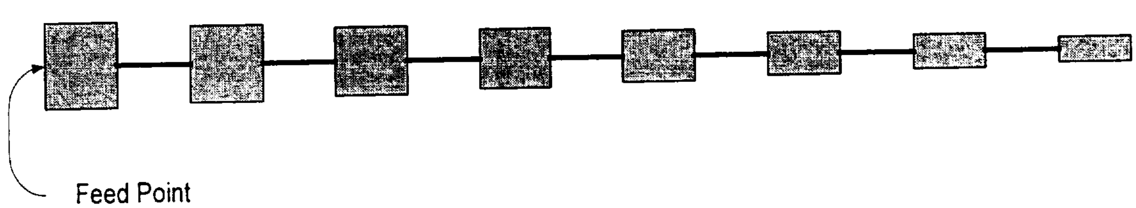

Figure 1: A subarray with 8 elements

In this design, the array has uniform excitation and has straight sections of transmission lines between the elements. In each subarray patches vary in dimensions at a uniform ratio to produce a very low beamwidth. The antenna is center fed at two points (one for each half of the array) with a 180° phase difference between the two subarrays.

2.2 Selection of substrate

The radiation efficiency of the antenna is determined primarily by the substrate permittivity and thickness [7]. In all the designs presented Rohacell foam with a permittivity of 1.08, with the commercially available thickness of 12.7mm was used as the substrate. The microstrip antenna was etched on RT duroid material RO 3003 made by Rogers Corporation with a permittivity of 3.0 and then inverted on to the Rohacell to form an inverted antenna. This configuration results in reduced dielectric losses.

2.3 Design of the single element

The geometry of the single inverted patch is shown in Figure 2.

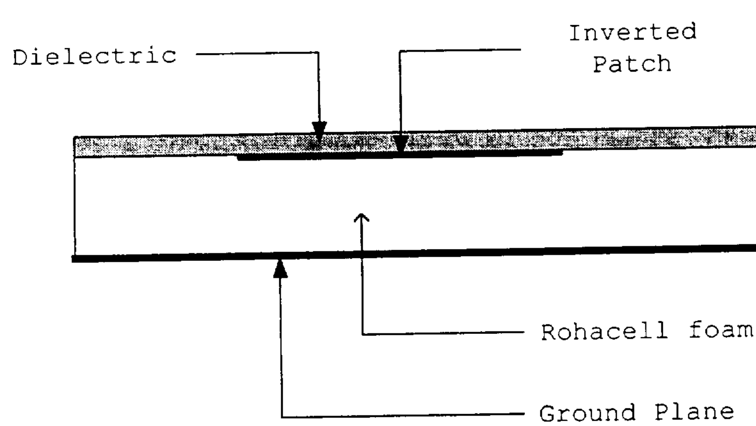

Figure 2: A single inverted patch antenna

The resonant length of a single patch microstrip antenna can be calculated from the formula as given below, [2,8]:

$$l = c \times (1 - 2 \cdot V_R) \times (2 \cdot F_R \cdot \sqrt{\varepsilon_{eo}})^{-1} - 2 \cdot \Delta l$$

Where, Δl = capacitive cutback factor

$$\Delta l = 0.412\, h \times (\varepsilon_e + 0.3)(w / h - 0.2674) \times (\varepsilon_e - 0.258)^{-1} (w / h + 0.8)^{-1}$$

c = speed of light, F_R = patch resonant frequency, V_R = variation in resonant frequency, ε_{eo} = effective dielectric constant of the patch without dielectric cover, l = patch length, w = patch width, and h = substrate thickness.

Width of the patch is given by the formula,

$$w = c \times (2 \cdot F_R)^{-1} \times [(\varepsilon_r + 1) / 2]^{-1/2}$$

The effective dielectric constant of a dielectric covered patch antenna is given by [8]:

$$\varepsilon_e = C_d / C_o$$

Where, C_o = capacitance/unit length without dielectric layer present, and

C_d = capacitance/unit length with dielectric layer present.

The capacitance per unit length of the dielectric-covered microstrip lines can be found using,

$$\frac{1}{C} = \frac{1}{4\pi\varepsilon_o} \int_0^{\infty} \left(\left[1.6 \frac{\sin(\frac{\beta w}{2h})}{(\frac{\beta w}{2h})} + 2.4 (\frac{\beta w}{2h})^{-2} \times \left[\cos(\frac{\beta w}{2h}) - \frac{2\sin(\frac{\beta w}{2h})}{(\frac{\beta w}{2h})} + \sin^2(\frac{\beta w}{4h}) \times (\frac{\beta w}{4h})^{-2} \right] \right] \right)^{-2} \times \left(\left[\varepsilon_{r1} \frac{\varepsilon_{r1} \times \tanh(\frac{\beta d}{h}) + 1}{\varepsilon_{r1} + \tanh(\frac{\beta d}{h})} + \varepsilon_{r2} \coth(\beta) \right] \right)^{-1} d\beta$$

Where β is the Fourier transform variable, ε_o is the permittivity of free space and d is the height of the superstrate.

The length of single patch obtained from the above empirical formula is 104 mm and the width of the patch is 87.1 mm. The length and width of the patch thus obtained is optimized using IE3D to match a 50Ω coaxial feed. This patch serves as the first (feed) element in each subarray.

2.4 Design procedure for the sixteen element array

The single patch described above is the first element of each of the eight element subarray and is fed with a coaxial probe. The dimension of the element as obtained for a 50Ω match is L=92.65 mm and W=84.9 mm. The other elements of the array have widths that decrease with a uniform ratio and are connected to each other by a half wavelength microstrip line. The final design of the two subarrays with decreasing patches is shown in Figure 3. The total length of the array is approximately 9.6 feet.

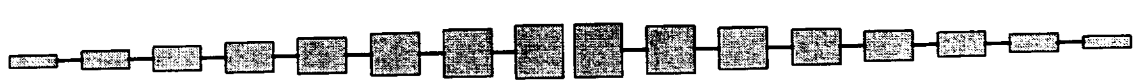

Figure 3: The two subarrays forming the 16 element array

2.5 Foldability of the antenna array

In order to make the array foldable the ground plane of each subarray was cut in two places beneath the microstrip lines to provide for the folds. The cut pieces are then connected together using flexible high conductive metallic tape to produce a continuous ground plane. To account for the discontinuity in the ground plane the computer simulation was done using strips in the regions where the tape was present accounting for the lower conductivity of the tape in comparison to the copper ground plane. The antenna geometry with ground plane modified are shown in Figure 4 and Figure 5. Figure 6 shows the folded antenna subarray.

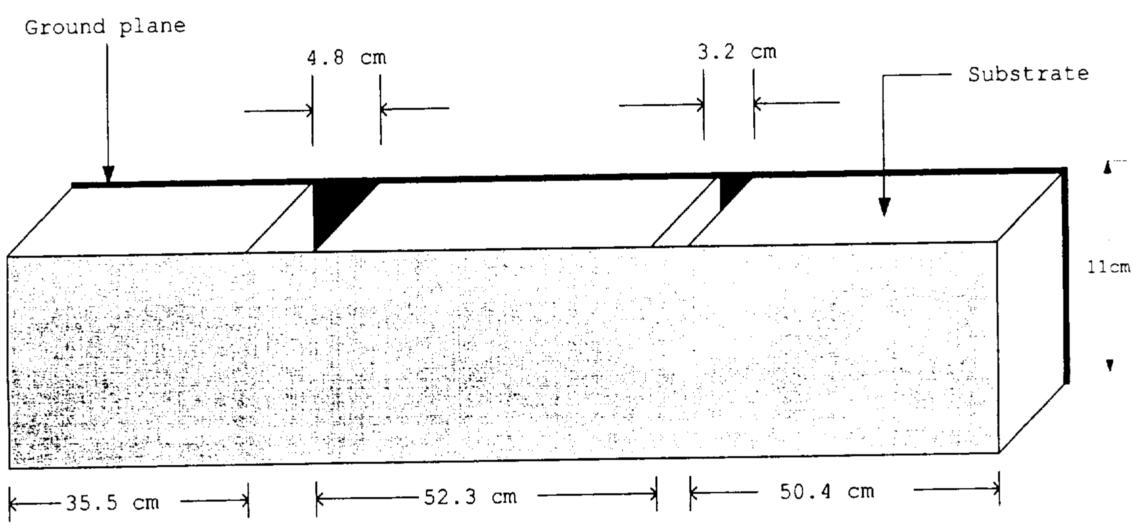

Figure 4: Antenna geometry for the foldable subarray

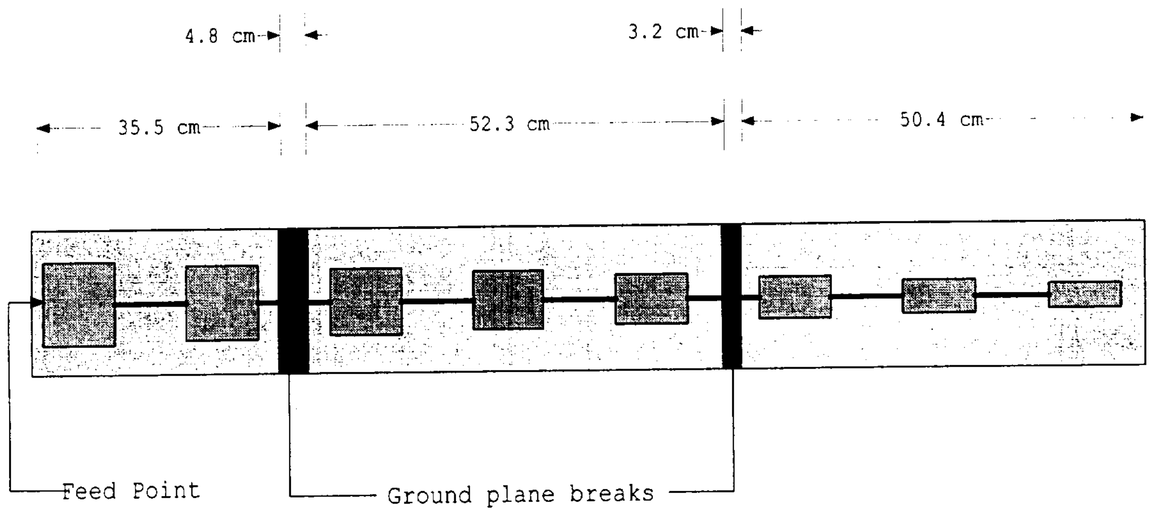

Figure 5: A subarray showing the location of the cuts in the ground plane

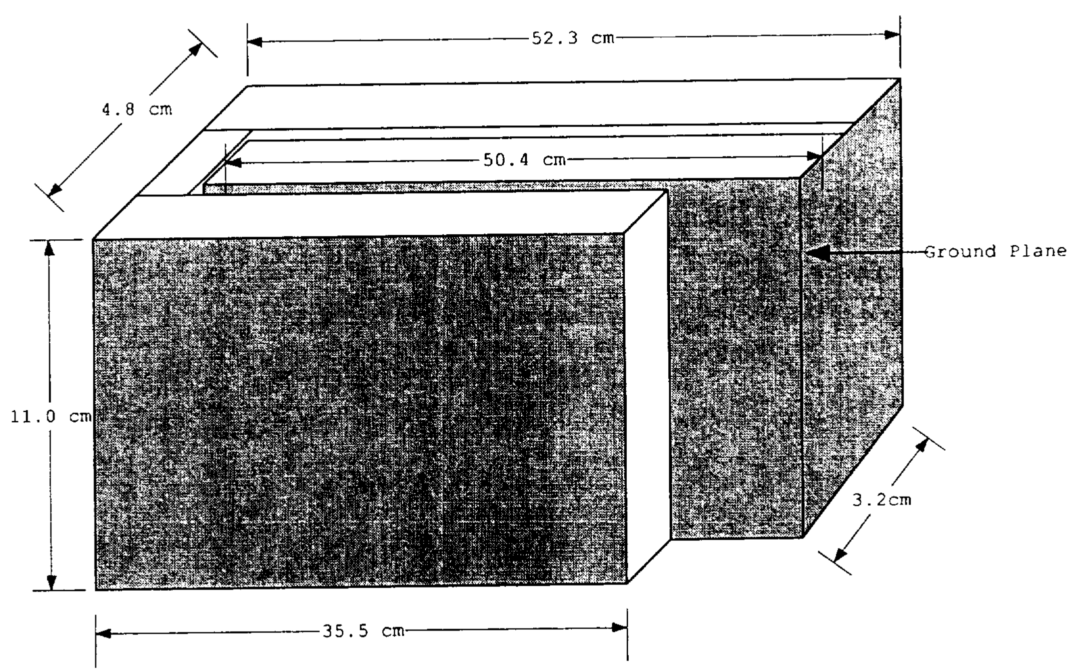

Figure 6: Folded antenna subarray

2.6 Simulated and Measured Results

The gain of the antenna under test is given by:

$$G_{test} = \frac{P_{test}}{P_{ref}} \cdot G_{ref}$$

or, $$G_{test}(dB) = G_{ref}(dB) + P_{test}(dB) - P_{ref}(dB)$$

The calculated gain of the antennas is given below,

Standard gain horn received power, P_{ref} = -25.0 dBm

Test antenna received power, P_{test} = -27.15 dBm

Gain of the standard horn, G_{ref} = 16.73 dB

Gain of the of the antenna in H-polarization is,

G_{test} = -27.15 + 25.0 +16.73 = 14.58 dB

Simulated directivity of the antenna for H-pol = 17.2 dB

Efficiency of the antenna = 14.58 – 17.2 = -2.62 dB

= 54.70%

Measured input impedance of each subarray was = 62.0 Ω.

The simulated input impedance was = 95.0 Ω

The simulated 2-D radiation pattern, the polar pattern, the 3-D mapped pattern are shown in Figure 7, Figure 8 and Figure 9 respectively for the 16 element antenna array with a continuous ground plane.

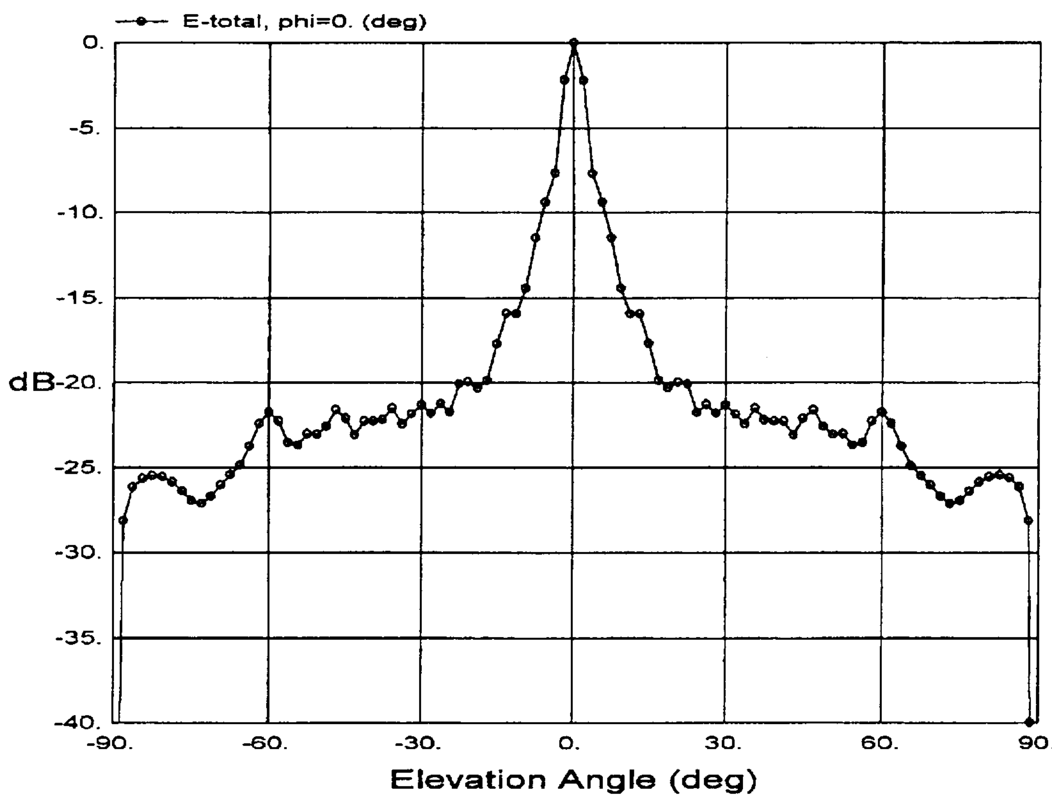

Figure 7: Simulated 2-D radiation pattern of the sixteen element array without cut in the ground plane

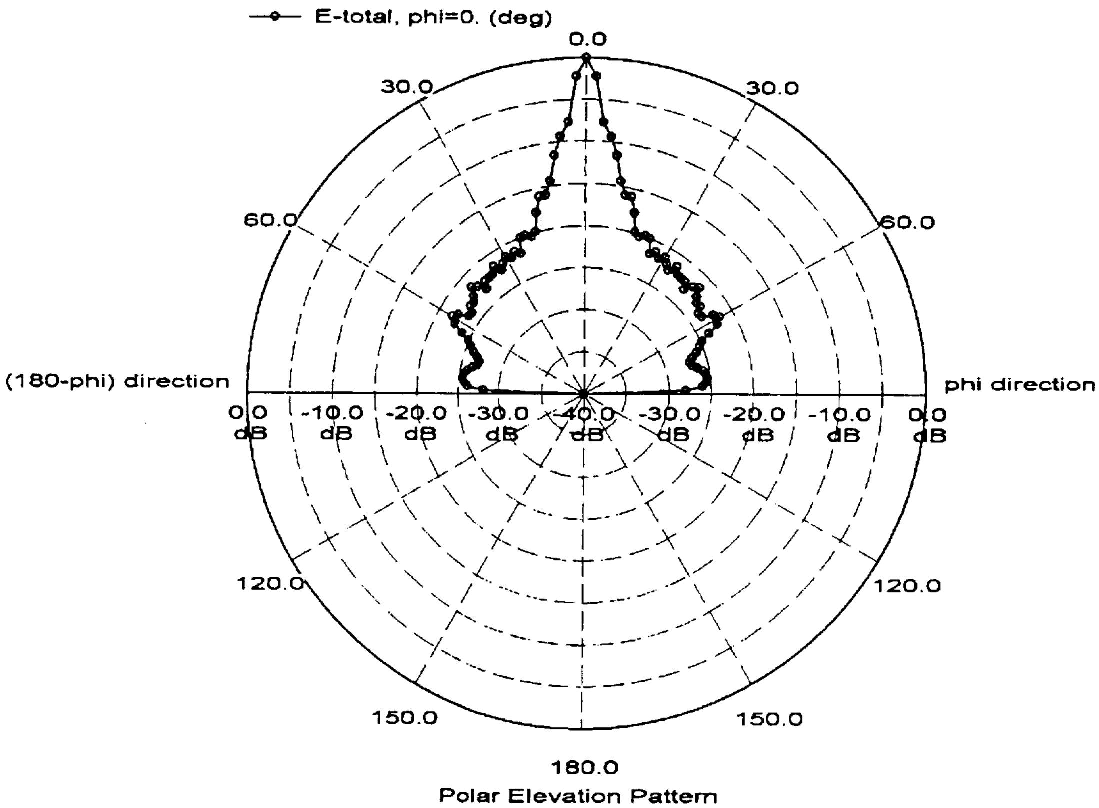

Figure 8: Simulated polar pattern of the sixteen element array without cut in the ground plane

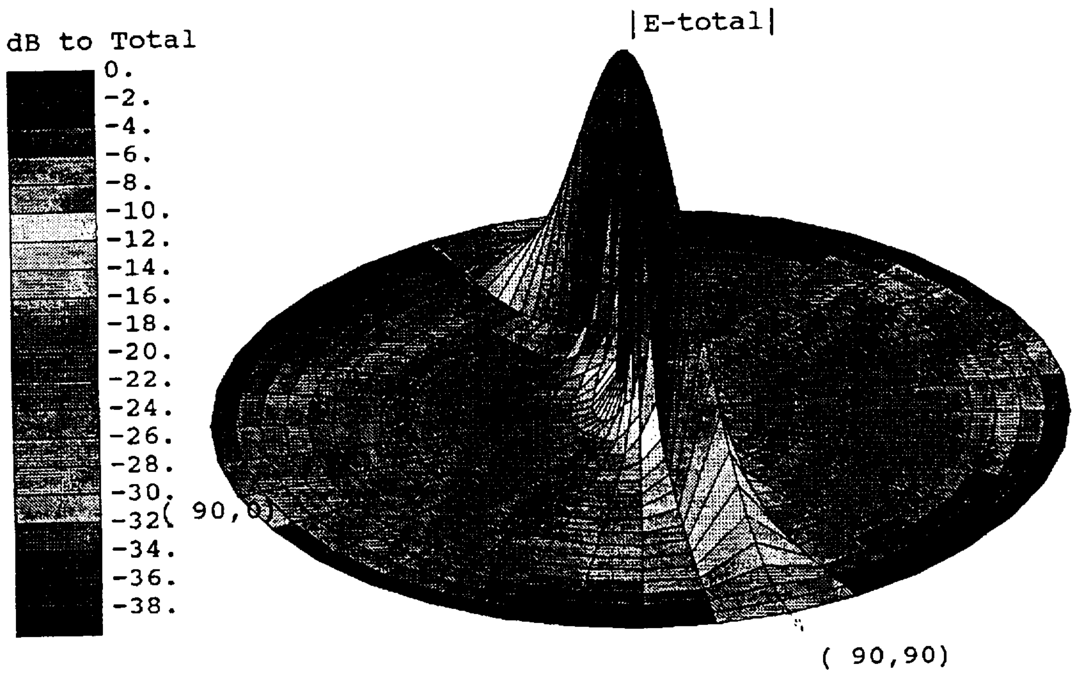

Figure 9: Simulated 3-D mapped pattern of the sixteen element array without cut in the ground plane

The antenna radiation pattern was measured in an outdoor test range in facilities at Technical Systems Associates (TSA) in Orlando with the frequency of 1.413 GHz. Figure 10 shows the comparison between 2-D simulated and measured radiation patterns for the foldable 16 element antenna array. The two patterns show a close agreement.

From the patterns we can see that the array has a narrow 3dB beamwidth of 4.3°, 10dB beamwidth of 18° and low side lobe levels below 15 dB as required in the design.

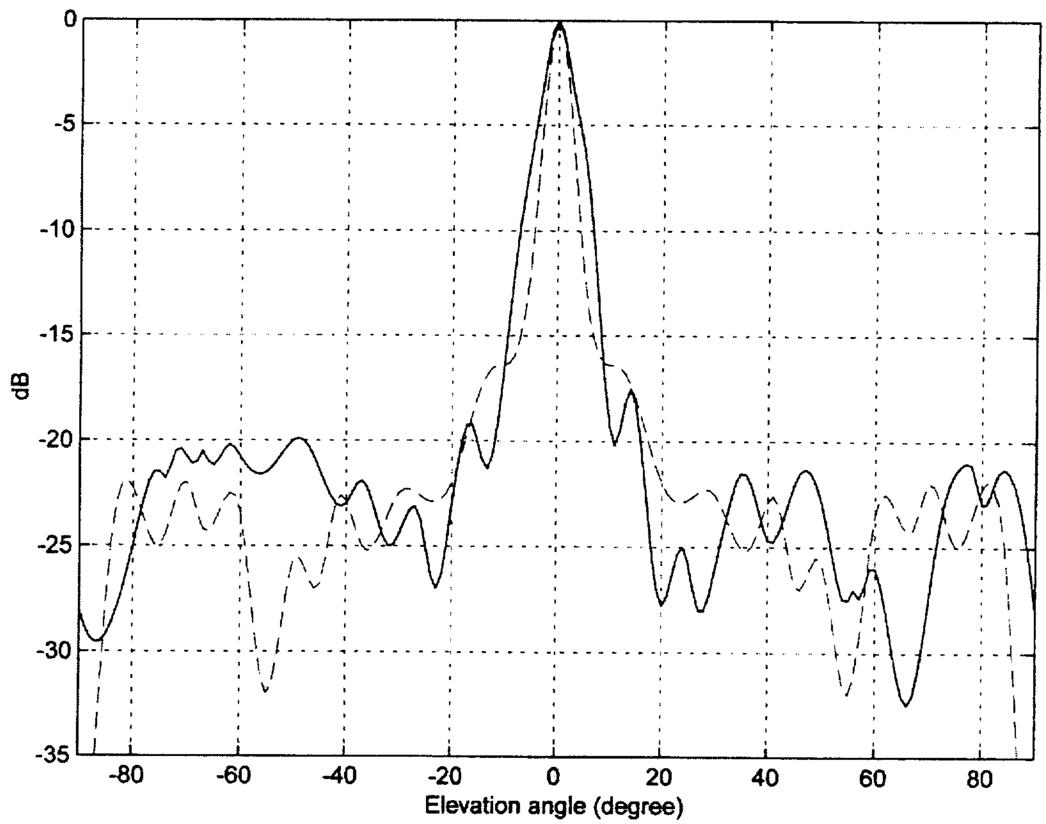

________ Measured radiation pattern

--------- Simulated radiation Pattern

Figure 10: Simulated and measured radiation pattern of the foldable 16 element antenna array

2.7 Design 2

In the previous design the antenna was not well matched to the probe so a different approach was taken to achieve a linear polarized antenna array which has better matching. The configuration shown in Figure 11 produces directive beam on broadside and is closely matched to the 50Ω probe. In this design the antenna has two equal subarrays composed of four elements each. Each subarray has patches of same width but varying lengths unlike the previous design where the width was varied and the length kept same.

In this design a pair of patches of same width and different length was taken as one block and matched to the feeding probe. Each subarray consists of two of these pairs (blocks) and is matched to 50Ω probe. The two subarrays are fed at the center 180° out of phase.

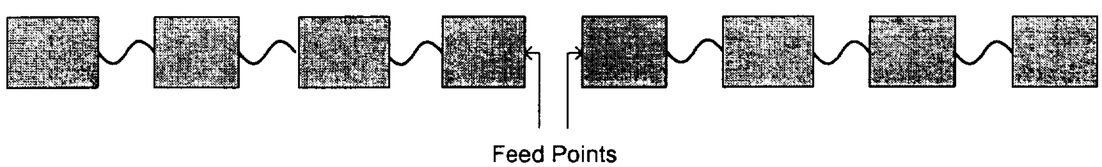

Figure 11: Eight element antenna array

2.8 Eight element design

In this array design which has uniform excitation, curved transmission lines are used. The half wavelength long connecting microstrip lines are curved to bring the patches closer to each other and reduce the grating lobes. The single element design procedure is as described in Section 2.3 with a design frequency of 1.413 GHz. The IE3D simulation software package was used to arrive at the patch dimensions for a 50Ω match. The dimension of the pair of patches obtained with IE3D is, L = 93.2 mm, W = 77.1 mm for the first patch and L = 100.2 mm, W = 77.1 mm for the second patch. The total length is around 4 feet.

2.9 Results

Input Impedance and return loss:

The simulated input impedance and return loss of the 8 element array is shown below,

Frequency(GHz)	Re[Z(1,1)]	Im[Z(1,1)]	dB[S(1,1)
1.000	12.58	131.60	-0.553
1.333	172.30	10.50	-8.112
1.400	71.62	-15.16	-16.95
1.413	56.75	-5.54	-18.93
1.500	24.24	56.75	-3.358
1.667	92.54	92.09	-4.58
2.000	33.60	179.60	-0.7275

The simulated directivity of the array is 15 dB.

The simulated 2-D radiation pattern, polar pattern, 3-D mapped pattern and return loss for the eight element array are shown in Figure 12, Figure 13 and Figure 14 and Figure 15 respectively. The return loss was –19dB at the design frequency indicating a good match. The pattern has a wider 3dB and 10dB beamwidth of 14.8° and 30° as compared to 4.3° and 18° obtained with the first design. The pattern does not have distinct side lobes, though the pattern falls below –15dB about 30° away from the main lobe.

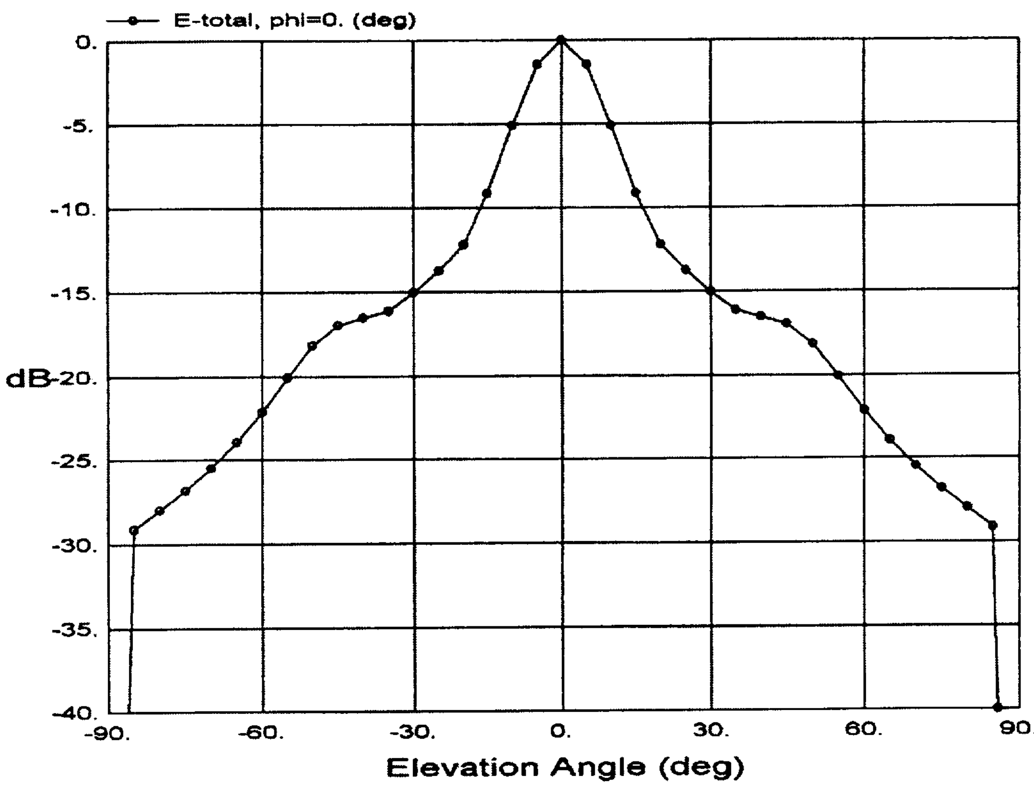

Figure 12: Simulated radiation pattern of the eight element array

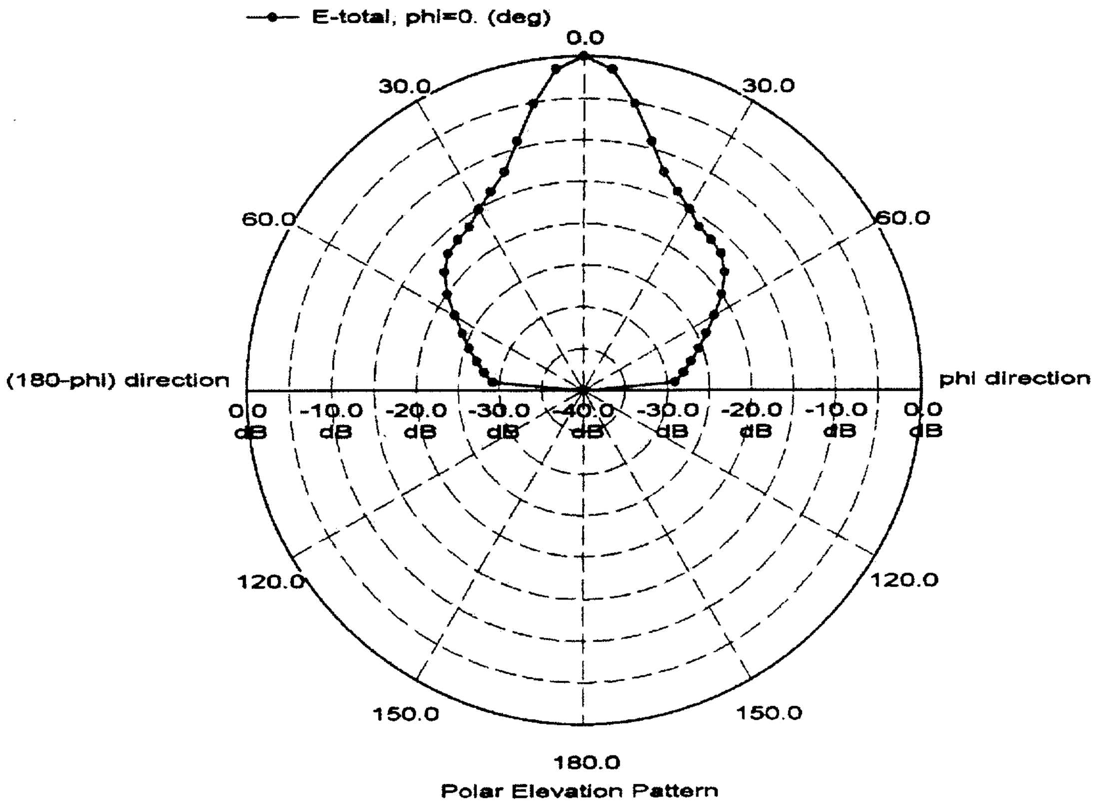

Figure 13: Simulated polar pattern of the eight element array

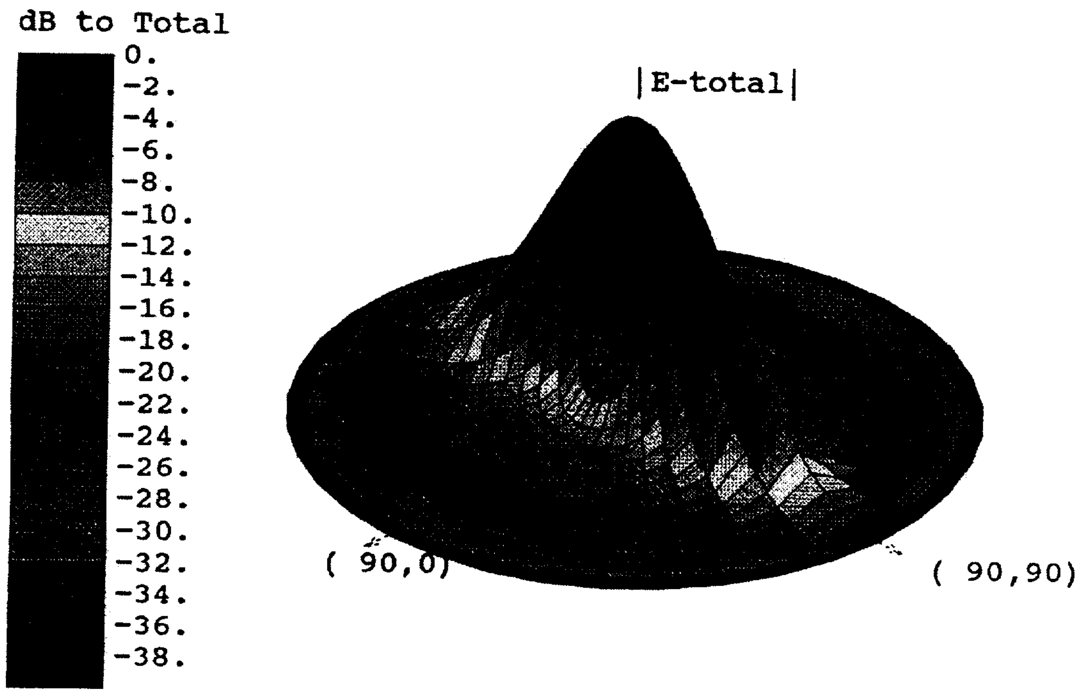

Figure 14: Simulated mapped pattern of the eight element array

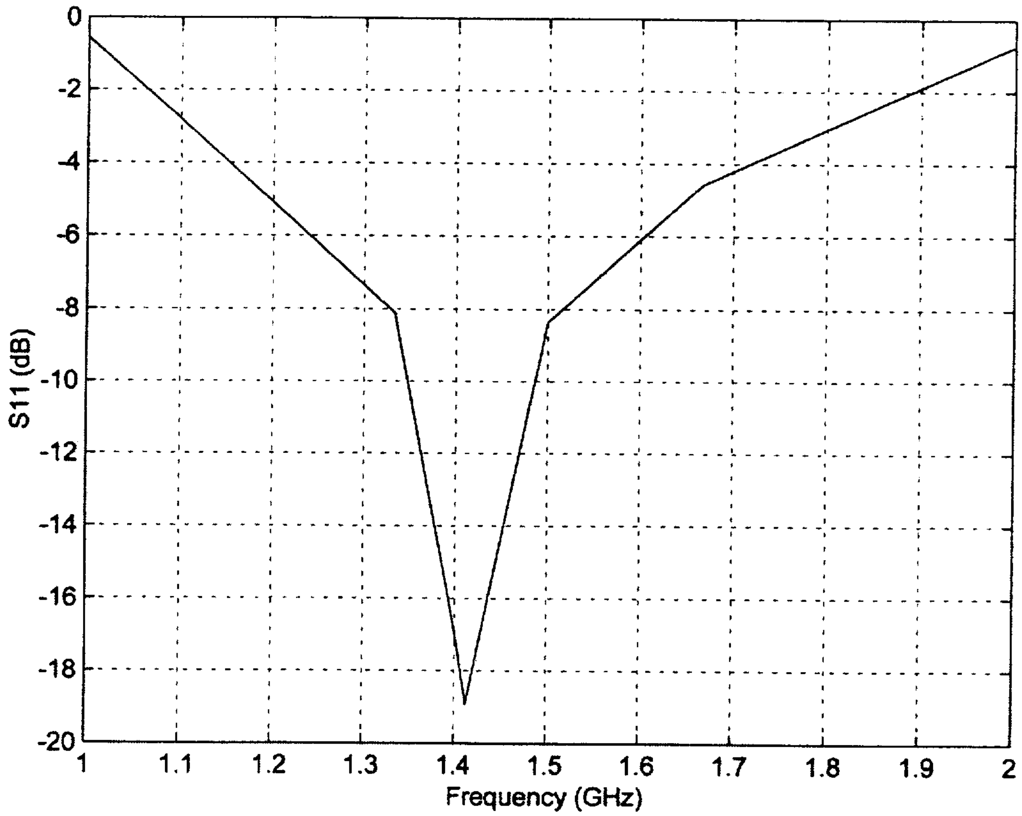

Figure 15: Simulated return loss of the eight element array

CHAPTER 3

3.0 Design of a dual polarized microstrip array

Dual polarized microstrip antennas have become very popular in remote sensing radar applications, primarily because of the features such as light weight, compactness and conformability. Several techniques for obtaining dual polarization have been developed and described in [9-15]. In antenna arrays with the same aperture and elements shared by two polarizations, there will be cross talk between the two polarization ports. This is due to poor isolation and high cross polarization levels, which are the result of higher order modes that occur in the patch cavity. In [10], for a linearly polarized array, a single feed on each patch of paired elements with opposite feed locations and opposite phases was used. For reducing the cross polarization a method has been described in [15] where two feeds were used to achieve dual polarization.

The layout of patches shown in Figure 16 was designed for achieving dual linear polarization. The design goal is to achieve higher directivity for both polarizations and lower side lobe level in both planes.

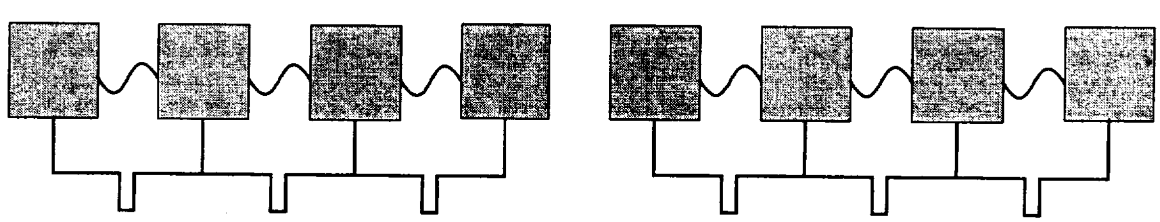

Figure 16: Eight element array for dual polarization

In this design, a series feed for horizontal polarization (H-pol) and corporate feeding for vertical polarization (V-pol) were used. For the H-pol the antenna is center fed at two points at the first element of each subarray with coaxial probes. A 180° phase difference is introduced between the two subarrays to produce highly directive beam on broadside. For the V-pol the antenna is fed by coaxial probes with microstrip lines at two points, one for each subarray. The two ports for V-pol are fed with same phase to produce highly directive beam on broadside of the antenna.

3.1 Design procedure for the eight element antenna

The dimensions obtained for the single patch is as described in Section 2.3 were slightly modified for a 50Ω match for use in this array design. Using IE3D the dimensions obtained are L = 92.7 mm and W = 86.7 mm. For the H-pol the dimension of the patch is obtained such that it is matched to the 50Ω probe and the feed arrangement is shown in Figure 17. In the array, the patches are connected with half wavelength long curved lines to reduce the grating lobes. The patches are closer but the electrical separation is equal to half wavelength. For the V-pol, a microstrip line is connected to the patch and the input impedance of the patch at the thin microstrip line is 200Ω. The structure of single patch for V-pol is shown in Figure 18. When the four patches of the subarray are connected in parallel with the half wavelength lines, the subarray produces a 50Ω impedance at the feed. The final arrangement for the H-pol feeding is shown in Figure 19 and for the V-pol feeding in Figure 20.

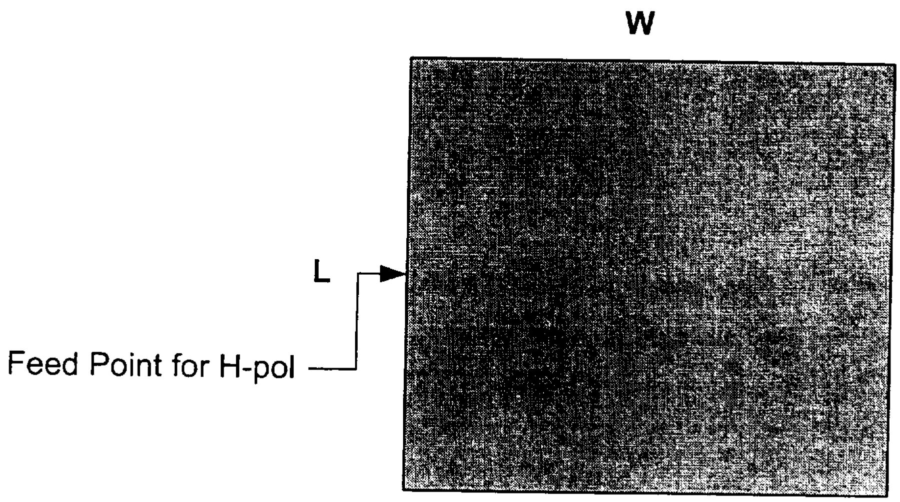

Figure 17: Layout of a single patch for H-polarization

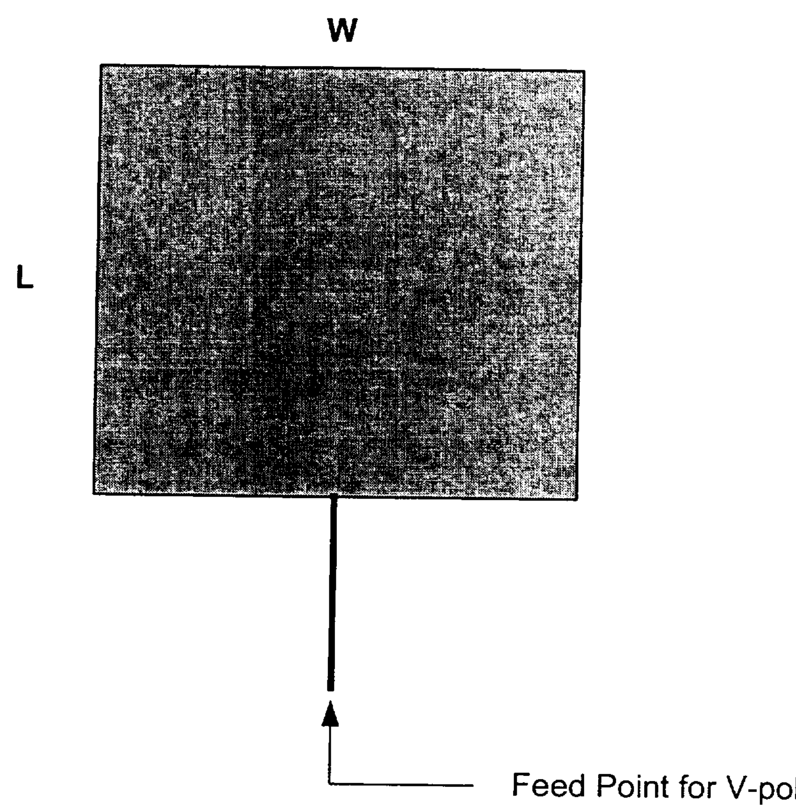

Figure 18: Layout of a single patch for V-polarization

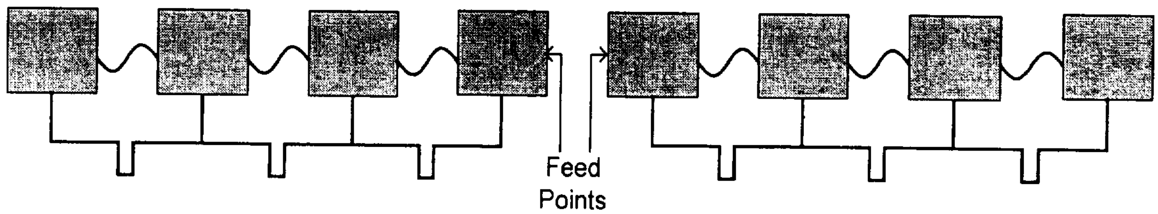

Figure 19: Feeding technique for H-polarization

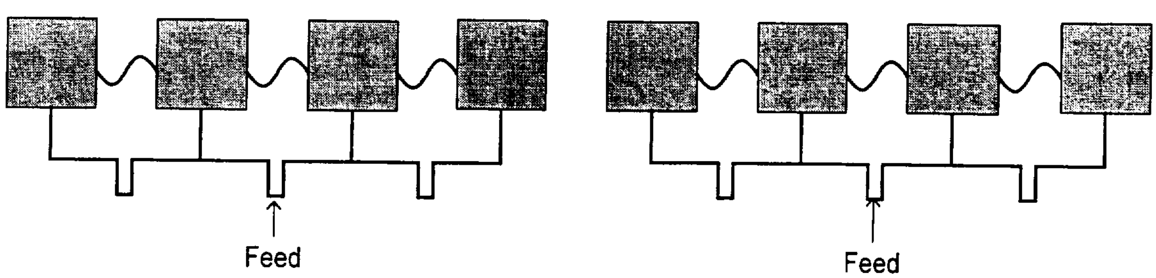

Figure 20: Feeding technique for V-polarization

3.2 Results

3.2.1 Input impedance and return loss

The simulated input impedance of the antenna array for H-pol was 59Ω and for the V-pol was 75Ω. The measured input impedance was 70Ω for H-pol and 55Ω for V-pol. The measured return loss for the antenna in V-pol is –26dB and for H-pol is –22dB.

3.2.2 Gain and efficiency measurement

Horizontal polarization:

Standard gain horn received power, P_{ref} = -23.3 dBm

Test antenna received power, P_{test} = -28.1 dBm

Gain of the standard horn, G_{ref} = 16.73 dB

Gain of the of the antenna in H-polarization is,

$G_{test} = -28.1 + 23.3 + 16.73 = 11.93$ dB

Simulated directivity of the antenna for H-pol = 14.1 dB

Efficiency of the antenna = 11.93 – 14.1 = -2.17 dB

= 60.67%

Vertical polarization:

Standard gain horn received Power, P_{ref} = -23.3 dBm

Test antenna received power, P_{test} = -27.5 dBm

Gain of the standard horn, G_{ref} = 16.73 dB

Gain of the of the antenna in V-polarization is,

$G_{test} = -26.85 + 23.3 + 16.73 = 13.18$ dB

Simulated directivity of the antenna for V-pol = 16.0 dB

Efficiency of the antenna = 13.18 – 16.0 = -2.82 dB

= 52.23%

3.2.3 Simulated and measured radiation pattern

Figure 21, 22 and 23 show the simulated 2-D, polar, 3-D mapped radiation patterns for the H-pol and Figure 24 shows the comparison between measured and simulated 2-D radiation patterns for the H-pol. The measured pattern had some sidelobes beyond 90° which did not appear in the simulated pattern.

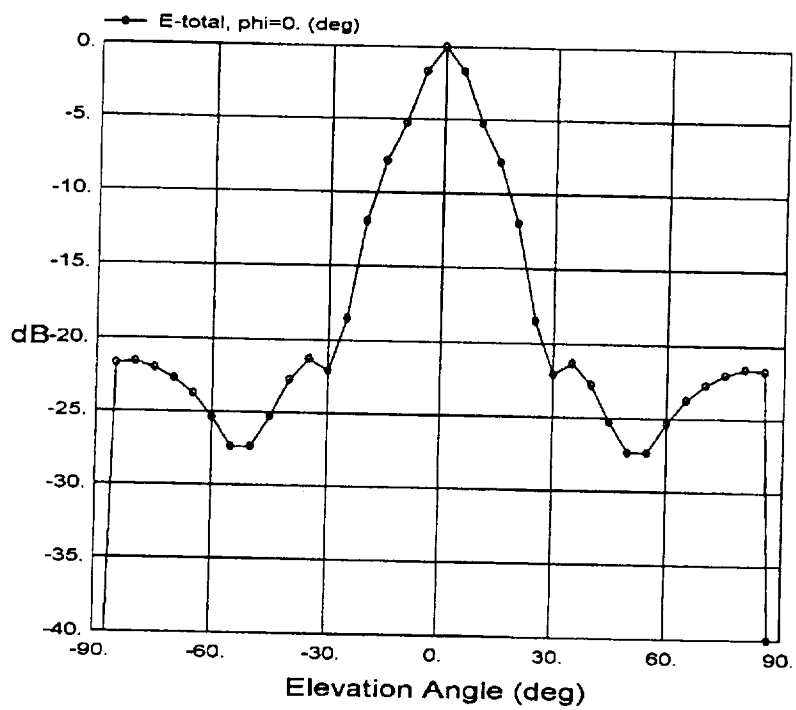

Figure 21: Simulated H-polarization radiation pattern

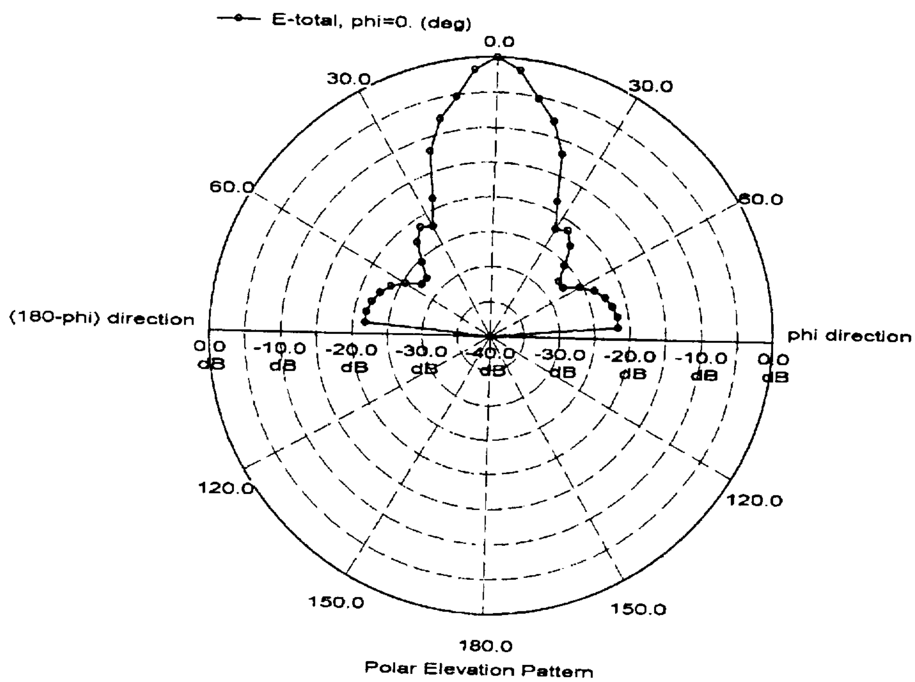

Figure 22: Simulated H-polarization polar pattern

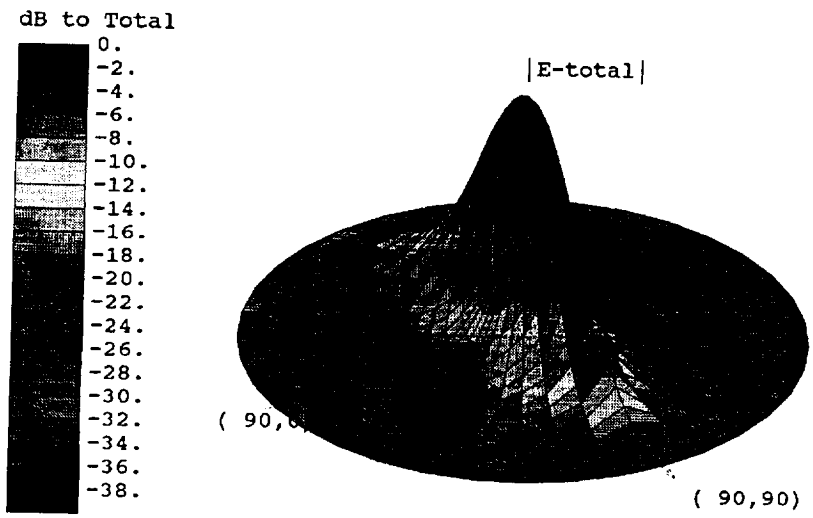

Figure 23: Simulated H-polarization 3-D mapped pattern

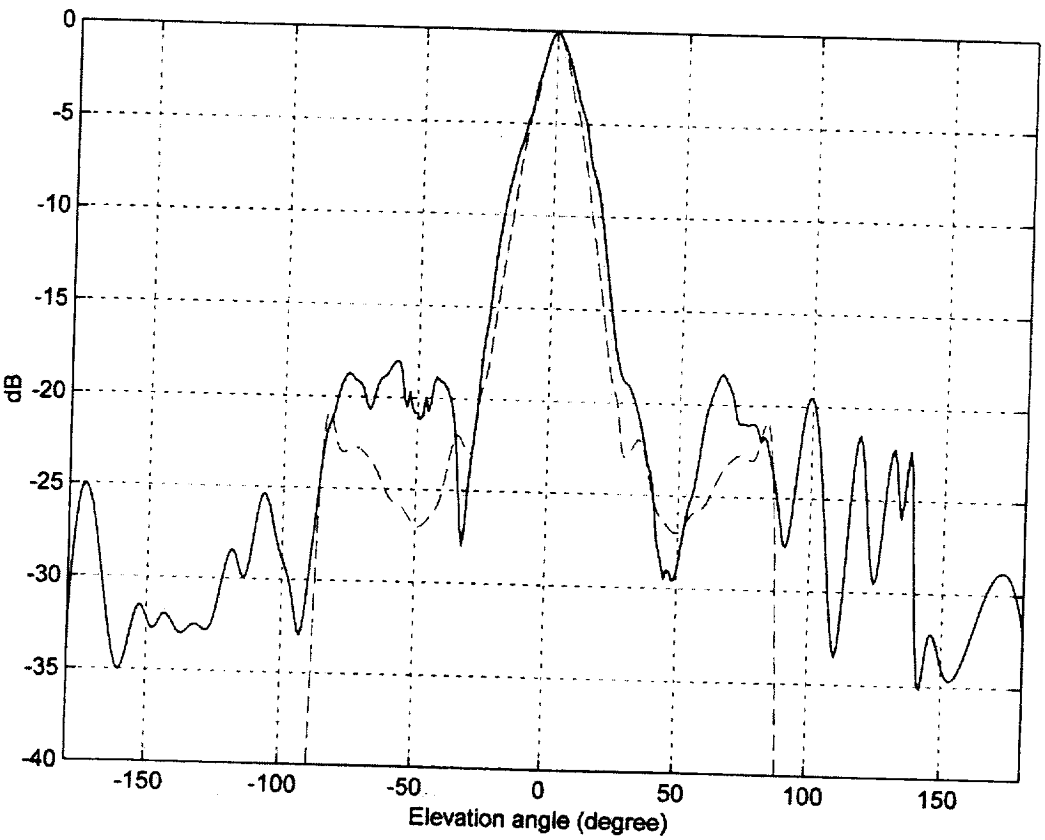

________ Measured pattern

---------- Simulated pattern

Figure 24: Measured and simulated H-polarization radiation patterns

Figure 25, 26 and 27 show the simulated 2-D, polar, mapped radiation patterns for the V-pol and Figure 28 shows the comparison between measured and simulated 2-D radiation patterns for the V-pol.

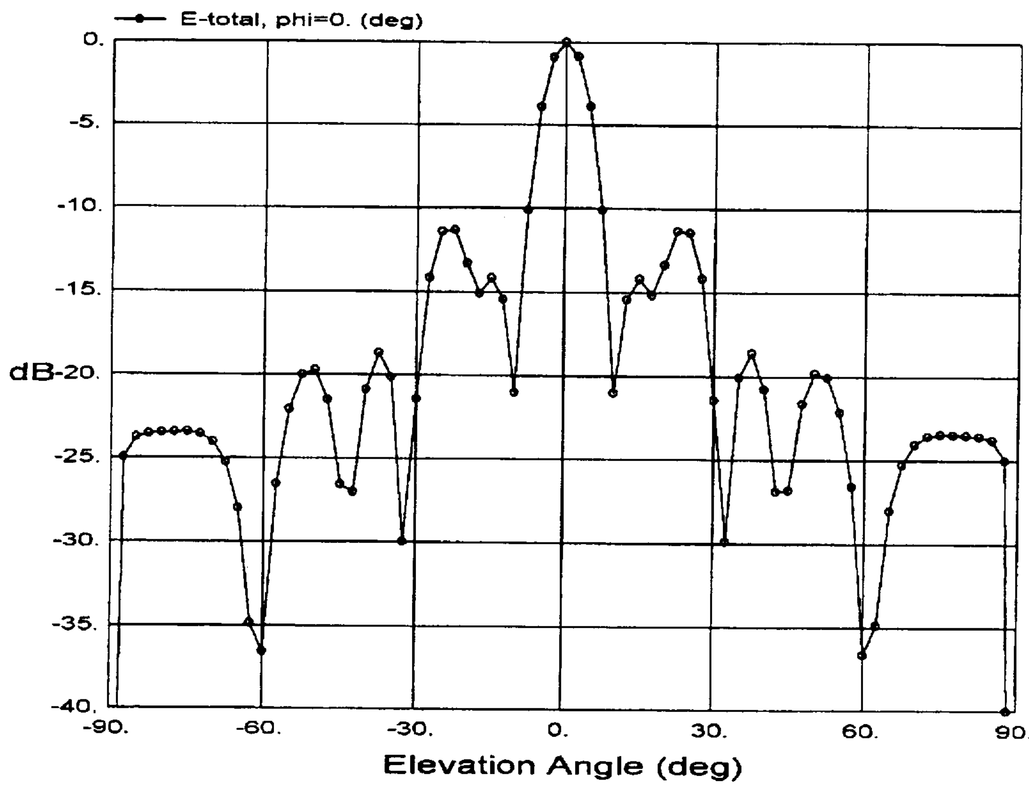

Figure 25: Simulated V-polarization radiation pattern

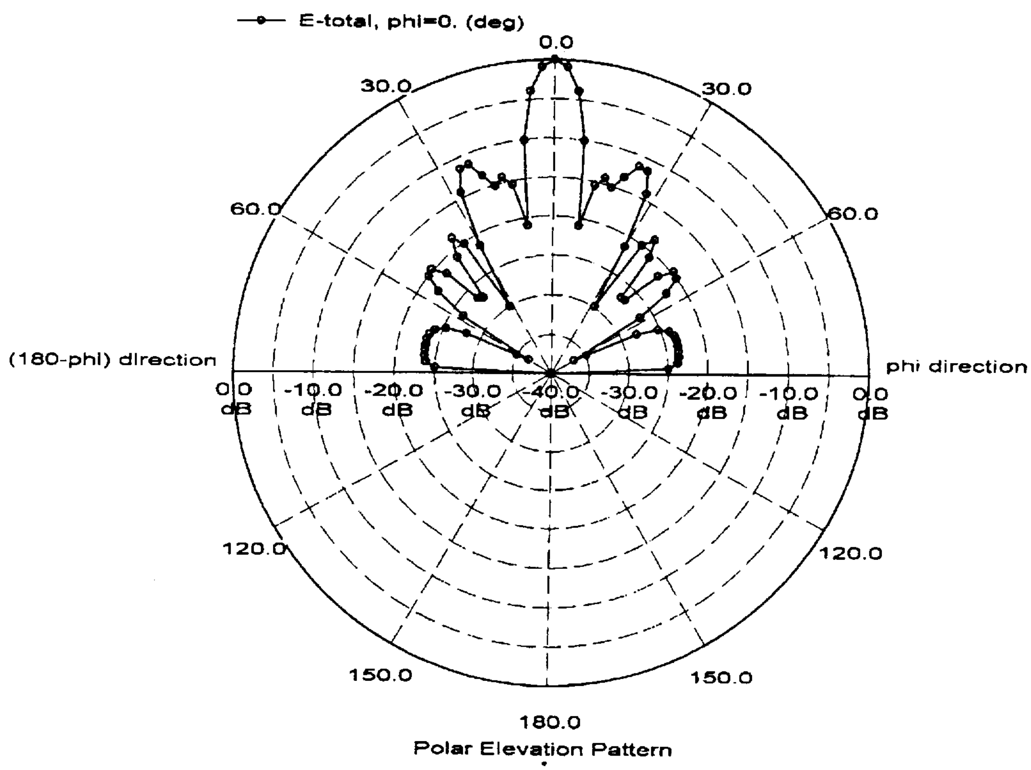

Figure 26: Simulated V-polarization polar pattern

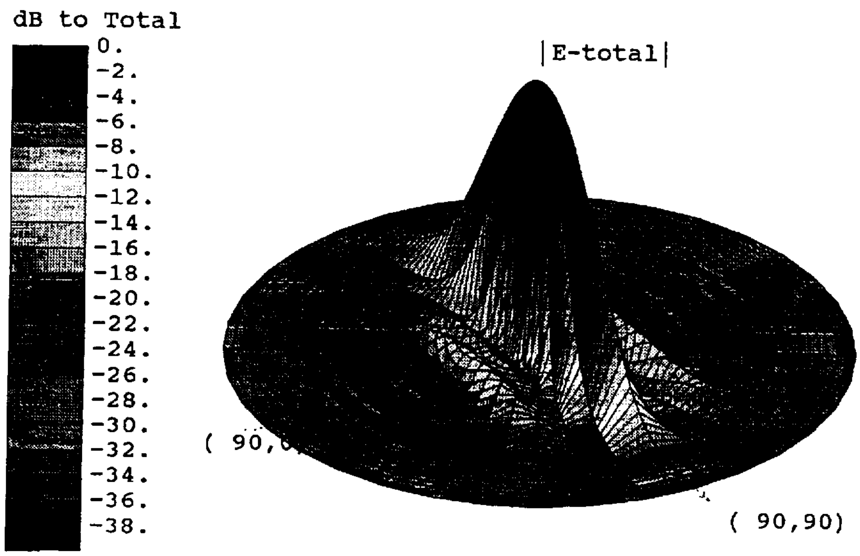

Figure 27: Simulated V-polarization 3-D mapped pattern

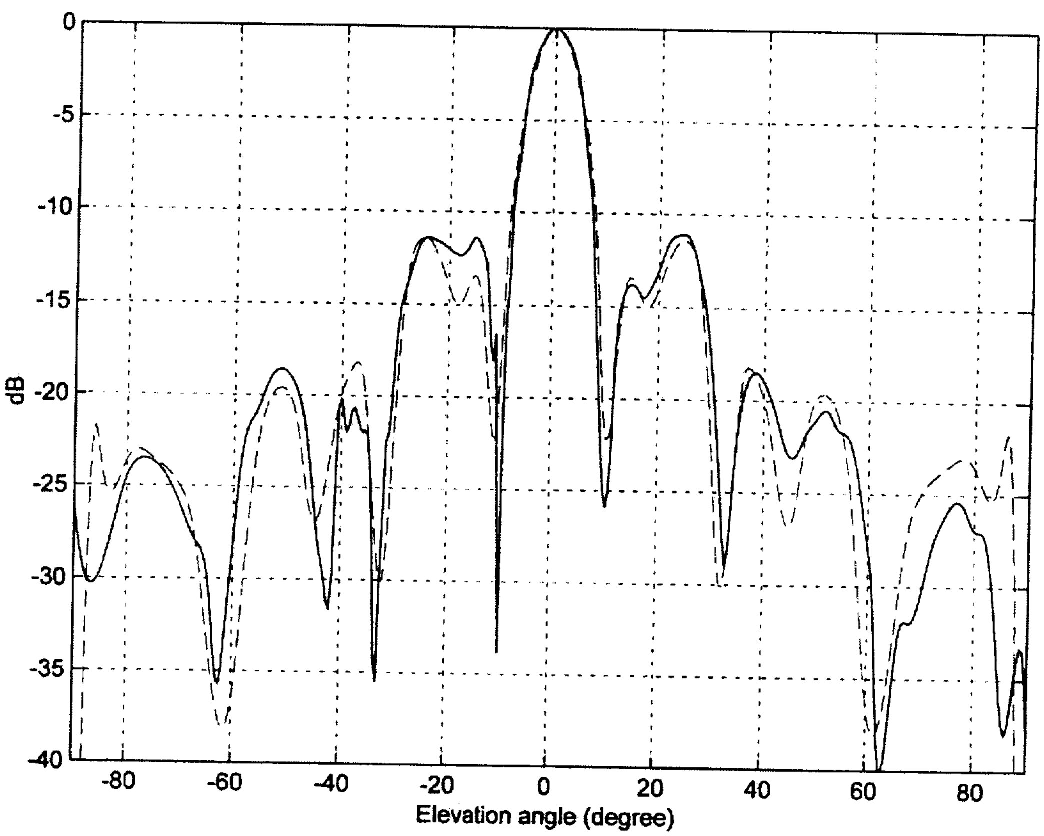

_______ Measured pattern

----------- Simulated pattern

Figure 28: Measured and simulated V-polarization radiation patterns

From the results we can see that the measured and simulated input impedance agree well and the 2-D radiation patterns shown in Figure 24 and 28 show excellent agreement between the measured and simulated results for the beamwidth and for the location and level of the side lobes.

CONCLUSION

The design of a series fed linearly polarized and a dual polarized antenna are presented. The array has to have low loss, a highly directive beam and low side lobe level. In addition the array should be foldable to allow transportation into space. The designs were simulated using the IE3D electromagnetic simulation tool. The design starts with obtaining the dimensions of a single microstrip patch at the design frequency of 1.413 GHz. An inverted microstrip antenna configuration is chosen because this configuration provides less dielectric and dispersion losses than the convention microstrip antenna configuration. RT Duroid RO3003 with a dielectric constant 3.0 was chosen as the dielectric cover for the inverted patches which were placed on Rohacell foam substrate with a dielectric constant of 1.08. In the first design, the patch width was reduced in constant ratio outward towards the end of the subarray to get higher directivity and low side lobes. The simulated and measured radiation patterns obtained agree very well. To get a better match at the feed, a different approach was taken by matching pairs of patches to 50Ω and using two of such pairs to form one subarray. In this approach the length of the patches were varied keeping the width the same.

For obtaining dual polarization the single patch dimension was optimized using IE3D and an almost square patch was used. The subarray consists of the four patches of equal dimension. Curved microstrip transmission lines were used to reduce side lobes for series feeding for the horizontal polarization and a corporate feed network was used for the vertical polarization. The measured radiation patterns agree very well with the simulated patterns for both polarizations.

REFERENCES

[1] Metzler T., "Microstrip Series Arrays," Proceedings of The Workshop on Printed Circuit Antenna Technology, October 17-19, 1979.

[2] Mahbub R.,"Design of a foldable series fed microstrip array antenna for radiometric applications," University of Central Florida, Orlando, Florida, 1998.

[3] Wu K.-L., Spenuk M., Litva J., Fang D. -G., "Feed network effects on the radiation pattern of series-fed microstrip antenna arrays," IEE Proceedings-H, Vol. 138, No. 3, June 1991.

[4] Kitazawa T. et al., "Planer transmission lines with finitely thick conductors and lossy substrates," IEEE Int. Microwave Symp. Digest, June 1991.

[5] Gauthier G. P., Courtay A., and Rebeiz G. M., "Microstrip Antennas on Synthesized Low Dielectric-Constant Substrates," IEEE Trans. On Antennas and Propagation, Vol. 45, No. 8, August 1997.

[6] Zealand Software Inc.

[7] Splitt G. and Davidovitz M., "Guidelines for design of electromagnetically coupled microstrip patch antennas on two-layer substrates," IEEE Trans. Antennas Propagation, vol. 38, pp. 90-94, July 1990.

[8] Bancroft R., "Accurate Design of Dual – Band Patch Antennas," Microwave & RF, September, 1988.

[9] Levine E. and Shtrikman S., "Experimental comparison between four dual polarized microstrip antennas," Microwave and Optical Technology Letters, vol. 3, pp-17-18, January 1990.

[10] Huang J., "Low cross-pol linearly polarized microstrip array," IEEE AP-S International Symposium Digest, pp-285-288, May 1982.

[11] Maci S., Gentili G. B. and Avitabile G., "Single layer dual frequency patch antenna," Microwave and Optical Technology Letters, vol. 29, no. 16, pp-1441-1443.

[12] Maci S., Gentili G. B., Piazzesi P. and Salvador C., " A dual band slot loaded patch antenna," IEE Proceedings-H, vol. 142, pp-225-232, 1995.

[13] Huang J., "Dual Polarized Microstrip Array with High Isolation and Low Cross Polarization," Microwave and Optical Technology Letters, vol. 4, no. 3, pp-99-103, February 1991.

[14] Huang J., Lou M., Feria D. and Kim Y., "An Inflatable L-band Microstrip SAR Array," IEEE AP-S International Symposium Digest, pp-2100-2103, 1998.

[15] Zawadzki M., and Huang J., "A Dual Polarized Microstrip Sub Array Antenna for an Inflatable L-band Synthetic Aperture Radar," IEEE AP-S International Symposium Digest, pp-276-279, July 1999.